Low-Cost Tracer Gas Sensor for Building Ventilation

Journal of Physics:
Conference Series

PAPER • **OPEN ACCESS**

Low-Cost Tracer Gas Sensor for Building Ventilation

To cite this article: V Gentile and M Perino 2025 *J. Phys.: Conf. Ser.* **3140** 092001

Journal of Physics: Conference Series **3140** (2025) 092001 doi:10.1088/1742-6596/3140/9/092001

Low-Cost Tracer Gas Sensor for Building Ventilation

V Gentile[1*], M Perino[1]

[1] Politecnico di Torino, C.so Duca degli Abruzzi 24, 10129, Italy

*vincenzo.gentile@polito.it

Abstract. The accurate assessment of Indoor Air Quality is crucial for occupant health, yet traditional methods for evaluating ventilation rates, such as tracer gas techniques using photoacoustic spectroscopy (PAS), face limitations in cost, logistics, and response time. This study presents the development and validation of a low-cost, fast-response sensor system for tracer gas measurement, capable of detecting multiple gases. The sensor employs a Non-Dispersive Infrared (NDIR) detector with wireless communication based on the asynchronous Bleak protocol, enabling spatially resolved IAQ monitoring. Laboratory validation using SF_6 as tracer gas in a small volume of 40 liters and against the PAS reference device demonstrated an accuracy within ±20% for ventilation rates between 1 and 7 air changes per hour (ACH). Unlike PAS, which provides one measurement per minute, the low-cost sensor captures up to 50 readings per second, offering superior tracking of transient ventilation events and dynamic IAQ variations. The results suggest that this system provides a practical alternative for real-time IAQ monitoring, supporting energy-efficient and health-conscious building management.

1. Introduction

Maintaining good Indoor Air Quality (IAQ) is essential for occupant health and well-being, particularly in preventing building-related illnesses and limiting the spread of airborne pathogens. Ventilation systems play a key role in IAQ by diluting and removing indoor pollutants—such as gases, vapors, and aerosols—through fresh, filtered air intake. However, except in the design and commissioning phase, the determination of fresh air in rooms (Air Changes per Hour, ACH) once a building is operational is rarely verified or continuously monitored. Instead, IAQ is often estimated using indirect indicators, such as CO_2 levels or other contaminant proxies.

Assessing fresh air distribution within a space is challenging, as it requires multipoint sampling, which involves complex logistics and expensive equipment. Direct measurement of air change rates can be achieved using tracer gas (TG) techniques. This method introduces a known quantity of a tracer gas (one that does not naturally occur indoors, typically the Sulfur Hexafluoride, SF_6) and tracks its concentration decay over time. The data is typically fitted to an exponential decay function, formulated according to boundary conditions, allowing for the precise determination of ACH under real operating conditions [1].

To detect and quantify gases accurately, photoacoustic spectroscopy (PAS) is commonly used. This technique relies on the conversion of light energy into sound energy. A collimated infrared light source, modulated at specific frequencies, interacts with targeted gas molecules, causing heating or cooling effects depending on quantum state excitation. This process generates pressure waves, which are detected by highly sensitive microphones. PAS systems are considered the quality standard for gas

concentration measurements, offering high precision even at extremely low concentrations (e.g., in the ppb range). However, their high cost and operational constraints limit their widespread use.

A major drawback of PAS is its slow response time, where each measurement usually takes between 20 and 60 seconds. This poses a significant challenge in highly ventilated environments, or in analyzing rapid transient correlated with human emissions, where gas concentrations change rapidly. In such cases, frequent sampling (every few seconds or even fractions of a second) might be required.

While PAS-based tracer gas measurements work well in single-room settings with moderate ventilation rates (e.g., 0.3 to 10 1/h), their application in multi-room environments with high air exchange rates is far more complex. In a multizone setup with N rooms, airflow assessment requires solving N(N+1) mass balance equations, meaning multiple tracer gases and simultaneous measurements at different locations are essential to quantify the interzonal airflow quantification. Hence multiple samplings of two different tracer gases are required, in different locations, with the closest temporal distance to avoid an unprecise representation of the mass exchange. This approach necessitate either multiple PAS devices or a multipoint sampler with a multi-gas monitor [2]. This makes multipoint, multi-gas tracer studies logistically challenging, particularly for field experiments [3][4][5]. However, the limitations on the multipoint is not only limited to the multizone. Indeed, in a single zone if multiple and simultaneous measurements are necessary, for example to verify the spatial effectiveness of ventilation devices (e.g., to determine the local age of air) the PAS will face the same issue logistics, or cost, or time responsiveness issues.

In addition, the standard PAS approach for ventilation measurements typically includes an auxiliary air pump that collects air from multiple locations within a room (or from different rooms in a multizone setup) providing a mixed concentration measurement. This method represents indeed an average volumetric concentration rather than a point-specific measurement. However, many building configurations and transient ventilation phenomena require multiple parallel measurements across different specific locations or for different gases. In these cases, PAS systems are often impractical due to logistical challenges and high costs, making continuous monitoring and realistic measurements in operational buildings difficult and challenging.

To address this limitation, this study presents the design, development and testing of a portable, fast-response and low-cost tracer gas measurement system that can be applied for multiple gases detection such as SF_6, CO_2, and propane.

2. Methodology

2.1. Description of the low-cost sensor

The low-cost sensor is designed for ease of use and affordability, employing wireless communication to deploy multiple units across building zones. This enables spatially resolved ventilation assessment and continuous monitoring without the need for physical connections via pipes or ducts. The sensor utilizes a Non-Dispersive Infrared (NDIR) gas detector, a simple spectroscopic device that detects specific gases exploiting a no dispersive element to narrow the light spectrum. To minimize signal drift and interference from operating conditions, the sensor includes a microprocessor that compensates for temperature variations, adjusting the voltage output based on gas concentration in a linear trend ranging from 0.2V to 3.3V for gas concentrations from 0 to full scale. Housed in a compact case (Figure 1b), the sensor incorporates a small fan to maintain airflow and prevent stagnation. It also measures temperature and relative humidity using the I2C-based SHT85 sensor from Sensirion. The NDIR signal is acquired and digitally converted at 12-bit resolution using a low-power SAMD21 Cortex®-M0 microprocessor (32-bit) with a sampling frequency of 50 Hz.

Data transmission is handled by the NINA-W102 radio module, operating in the 2.4 GHz Bluetooth frequency band for energy efficiency. The architecture uses a cross-platform protocol based on the Bluetooth Low Energy (BLE) library (Bleak, MIT license) in Python, enabling communication with BLE-capable central devices such as Raspberry Pi, PCs, or other BLE-enabled systems. The implementation follows an asynchronous API (asyncio) to ensure smooth data transmission at 100 Hz

without issues and from multiple devices. The architecture consists of multiple steps: first, scanning and connecting the peripheral device (the low-cost sensor) to a central unit (running the Python software); second, a discovery phase to identify services (e.g., the kind of information such as gas concentration, temperature, and humidity) and characteristics (data values); and third, a reading phase where sensor data is transmitted to the central unit at 50 Hz.

For standalone operation, the sensor requires an external battery. A 10,000 mAh, 5V power bank was used in our tests, providing uninterrupted operation for several weeks still maintaining the portability constraints. To validate the sensor architecture, we tested three SF_6 modules with different full-scale ranges—two at 500 ppm and one at 2000 ppm—to assess the impact of sensor sensitivity on measurement accuracy. The performance of the low-cost sensors was compared against a laboratory-grade PAS reference device.

2.2. Experimental setup for LCS validation

Figure 1a illustrates the experimental setup used to validate the low-cost SF_6 sensor, as shown in the images of Figures 1a and 1b. A 40-liter transparent test box was used, with one side connected to an external pressurized dry air circuit (<1 bar), simulating the fresh air supply in a room. The airflow was controlled using a mass flow controller, regulating the flow rate between 0 and 10 liters per minute. A 1 meter long nylon tube (6 mm inner diameter) connected the test box to the PAS reference device, the INNOVA 1512 from Lumasense. The test box had two additional openings: one for injecting a known quantity of SF_6 using a plastic syringe (each 5 mL injection corresponded to approximately 100 ppm once fully dispersed in the box) and another for exhausting the air, simulating ventilation. Inside the box, three low-cost sensors equipped with SF_6 sensing elements were placed, as shown in Figure 1b. The test began by injecting a known volume of SF_6 gas while all sensors (both PAS and low-cost sensors) recorded measurements. After allowing a few minutes for stabilization, fresh air was introduced at a fixed flow rate for the duration of the test. The experiment concluded when the SF_6 concentration, $C_{(t)}$, had decreased to approximately one-sixth of its initial concentration, C_0 (i.e., a 5-6 times reduction). This process was repeated three times to ensure test repeatability.

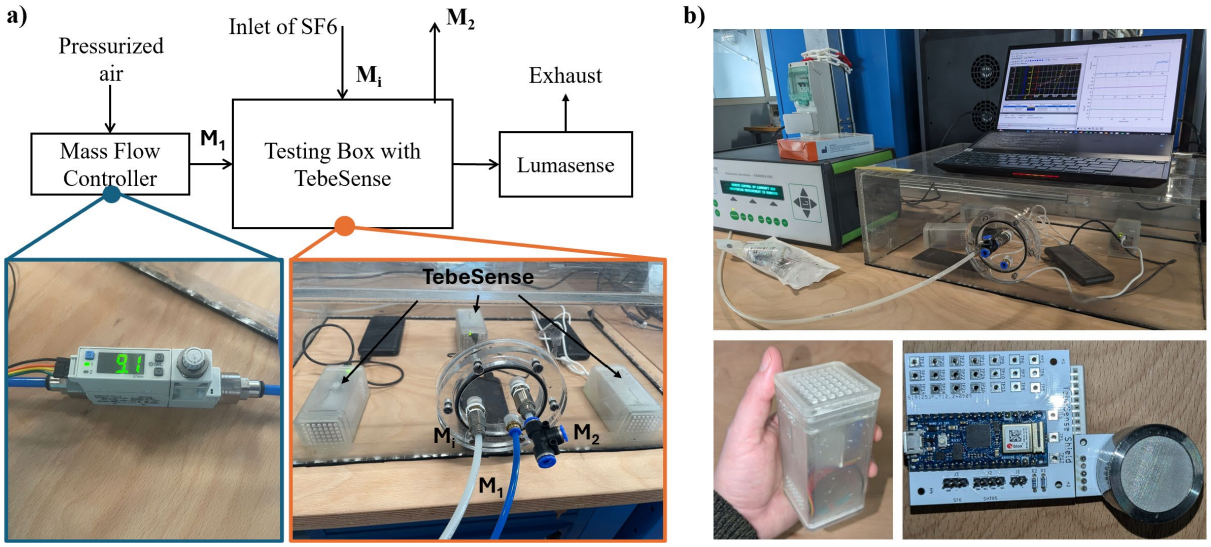

Figure 1. (a) Experimental setup with a mass flow controller and 3 TebeSense sensors. (b) Comparison of TebeSense and Lumasense devices, highlighting their size differences during testing.

2.3. Fitting with Decay model

Under ideal conditions, assuming no recirculation of exhaust air, the decay of a tracer gas (TG) in a single-room scenario follows a simple exponential function:

$$C_{(t)} = C_0 e^{-\lambda t} \quad (1)$$

Where: C(t) is the instantaneous SF_6 concentration; C_0 is the initial concentration; t is time in minutes; λ is the decay constant in 1/min. The experimental data were fitted using the least-squares error minimization method. This approach involves iteratively finding the decay constant λ and the initial concentration C_0, that minimizes the error function:

$$err = \sum_{j=1}^{N} [C_{(t)} - y_t]^2 \quad (2)$$

where y_t represents the instantaneous concentration measured by either the low-cost sensor or the PAS device at the same time as C(t). To optimize the error function, the Simplex Nelder-Mead algorithm was employed, with a residual tolerance threshold set at 10^{-8}, ensuring a highly accurate fit.

3. Results and Discussion

3.1. LCS versus Reference Lab Grade

Figure 2 presents an example of a decay test conducted simultaneously on the four different sensors used in the study. The red triangles represent the PAS device outputs, while the dots indicate data from the low-cost sensors: blue and orange correspond to the TEBE II and III sensors (both with a full scale of 500 ppm), while green represents the TEBE IV sensor (full scale of 2000 ppm). In particular, the plotted dots are only the average value out of the 50 values received from the wireless transmission of the low-cost sensors. Each plot also includes a dashed curve, which represents the fitted decay function obtained through an iterative algorithm. This algorithm identifies the two parameters, C_0 and λ, that minimize the error function in Equation 2 for each dataset. The identified parameters are reported within the graphs.

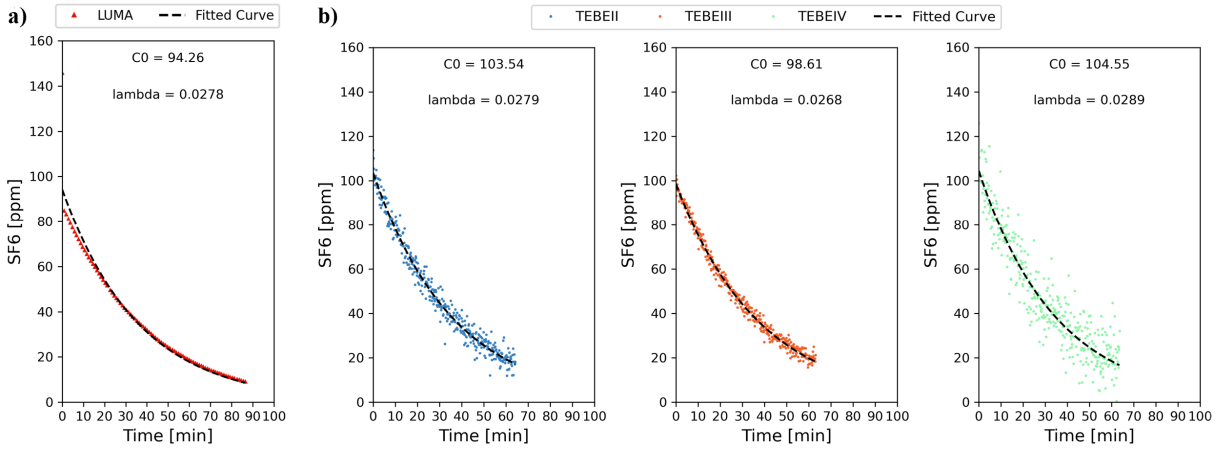

Figure 2. Results of the decay test and fittings with the exponential function for the reference lab grade sensor Lumasense (a), and the three low-cost sensors TEBE II, III, IV (b).

Table 1. Numerical results of the fitting the decay function with experimental data, and comparison with the fresh flow rate set in each experiment.

Fresh air flow rate	ACH	LUMASENSE		TEBEII		TEBEIII		TEBEIV		SF6 Decay tracing VS Mass flow controller			
		C_0	λ	C0	λ	C0	λ	C0	λ	Δ_{LUMA}	Δ_{TEBEII}	$\Delta_{TEBEIII}$	Δ_{TEBEIV}
L min^{-1}		ppm	min^{-1}	ppm	min^{-1}	ppm	min^{-1}	ppm	min^{-1}	%	%	%	%
1	1,5	85	0,026	103	0,028	98	0,026	104	0,028	2%	9%	4%	12%
1	1,5	91	0,026	111	0,028	105	0,027	103	0,033	2%	10%	8%	32%
1	1,5	94	0,028	106	0,027	101	0,028	102	0,035	10%	8%	10%	37%
2	3,0	104	0,059	110	0,055	100	0,059	107	0,070	17%	9%	16%	39%

2	3,0	86	0,051	103	0,059	102	0,056	74	0,055	0%	16%	11%	9%
1,9	2,9	76	0,049	83	0,060	83	0,061	82	0,052	3%	25%	27%	8%
2	3,0	63	0,053	63	0,076	66	0,070	55	0,057	5%	51%	39%	13%
3	4,5	78	0,080	63	0,091	73	0,080	70	0,078	6%	20%	6%	4%
3	4,5	59	0,067	65	0,069	77	0,073	68	0,085	-12%	-9%	-3%	12%
3	4,5	56	0,072	111	0,077	117	0,096	126	0,105	-5%	2%	27%	38%
5,2	7,9	68	0,112	59	0,156	73	0,150	74	0,166	-15%	19%	14%	26%
5,2	7,9	86	0,112	85	0,141	98	0,147	110	0,160	-14%	7%	12%	22%
5,1	7,7	99	0,112	101	0,160	122	0,162	129	0,159	-13%	25%	26%	24%
7,1	10,7	130	0,197	107	0,190	130	0,205	131	0,231	10%	6%	15%	29%
6,9	10,4	84	0,160	96	0,193	120	0,184	122	0,232	-8%	11%	6%	34%
7,2	10,9	64	0,168	57	0,192	84	0,167	83	0,220	-7%	6%	-8%	21%

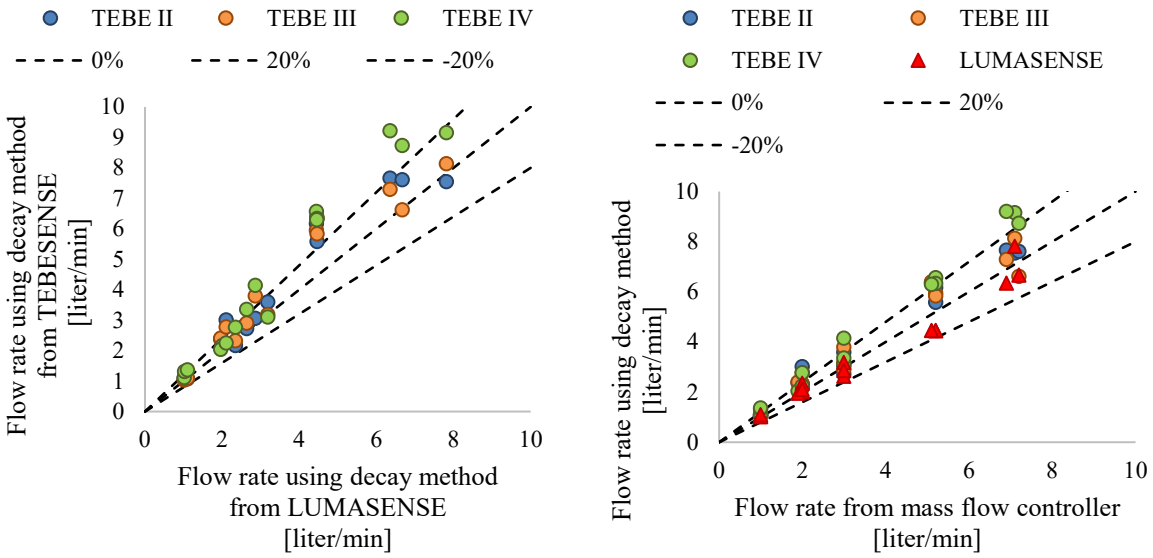

Figure 3. Results of the decay test and fittings with the exponential function for the reference lab grade sensor Lumasense (a), and the three low-cost sensors TEBE II, III, IV (b).

One key observation from the data is the difference in data density. Due to the higher acquisition frequency of the low-cost sensors compared to the PAS device, they provide more data points, but with greater dispersion. This effect is particularly evident for the low-cost sensor with the highest full-scale range, which exhibits the highest data dispersion. This trend was consistently observed across different experiments, with representative results summarized in Table 1 and compared in Figure 3.
Another important finding from the tests is the difference in how the fitted decay curve interpolates the available data. For the low-cost sensors, the dashed curve closely follows the average trend of the data points. However, in the case of the PAS device, there is a pronounced discrepancy between the model and the initial experimental data. This inconsistency can be attributed to the incomplete mixing of the gas in the early phase of the experiment, which affects the PAS readings more significantly than the low-cost sensors. While the PAS measures a volumetric average concentration, requiring time for the gas to fully mix and align with the decay model assumptions, the low-cost sensors capture a more localized decay within the test box. A key assumption of the decay model is that the tracer gas is perfectly and homogeneously mixed within the examined volume, which is not always immediately achieved in practice.

Figure 3 summarizes the complete experimental campaign through two comparative analyses. The left-side graph compares the fresh airflow rate (calculated by multiplying the decay constant λ by the

test box volume) as determined by the low-cost sensors versus the PAS device for the same test. The right-side graph compares the airflow rates from all sensors against the mass flow rate injected and controlled using the mass flow controller. The results indicate that, in most tests, the low-cost sensors overestimated the airflow rate compared to the PAS device. The degree of overestimation varied based on operating conditions and the final air change rate (ACH). The worst-performing sensor, TEBE IV, overestimated the PAS-detected flow rate by up to 40%. This discrepancy was primarily due to its high full-scale range, which was not well-suited to the low SF_6 concentrations used in the experiment. On the other hand, the low-cost sensors demonstrated an accuracy within ±20% of the reference mass flow controller values, particularly at higher flow rates. Notably, in the range of ACH values from 5 to 10, the PAS device exhibited a tendency to underestimate the flow rate, a trend that was not observed in the low-cost sensors.

4. Conclusion

In side-by-side comparisons with reference sensors, the low-cost sensor system demonstrated accuracy within ±20% of the benchmark measurements. In particular, low-cost sensors demonstrated an interesting consistency over the full range of measurement in terms of accuracy against the actual mass of fresh air injected in the testing box. A key advantage of our low-cost system is its high acquisition frequency: each sensor can capture up to 50 different concentration data points per second, enabling robust real-time tracking in environments with 1–7 ACH. In contrast, the reference PAS sensor provides only one concentration measurement per minute, limiting its responsiveness to fast changes in ventilation or contaminant levels. The rapid acquisition rate of the new sensor system also allows it to capture transient events common in highly ventilated environments (ACH>10), where fast fluctuations occur, and a high number of points are needed to accurately model the decay of tracer gases. The system's high data resolution also supports the identification and analysis of quick emission events, such as those arising from occupant activity. This capability enhances its applicability beyond static ventilation monitoring, enabling dynamic IAQ management by identifying and quantifying additional indoor contaminants in real time. Overall, the low-cost, high-frequency tracer gas sensor system provides a promising solution for ongoing IAQ management in diverse building environments, supporting energy-efficient and health-conscious building operations.

Acknowledgements

The research activity presented in this paper is done in a project funded under the National Recovery and Resilience Plan (NRRP), Mission 4 Component 2 Investment 1.3 - Call for tender No. 1561 of 11.10.2022 of Ministero dell'Università e della Ricerca (MUR); funded by the European Union – NextGenerationEU. Award Number: Project code PE0000021, Concession Decree No. 1561 of 11.10.2022 adopted by Ministero dell'Università e della Ricerca (MUR), CUP E13C22001890001, according to attachment E of Decree No. 1561/2022, Project title "Network 4 Energy Sustainable Transition – NEST".

References

[1] Etheridge, David W; Sandberg, M.; *Building Ventilation: Theory and Measurement*. (John Wiley & Sons, Ltd, Chichester, UK, 1996).
[2] Rulet C. -A. , Vamdaele L., Airflow patterns within buildings - Measurement techniques. Air Infiltration and Ventilation Centre - AIVC Technical, 1–23 (1991).
[3] Nazaroff, W. W. Residential air-change rates: A critical review. Indoor Air 31, 282–313 (2021).
[4] Liu, Y., Misztal, P. K., Xiong, J., Tian, Y., Nazaroff, W. W., Goldstein, A. H. Detailed investigation of ventilation rates and airflow patterns in a northern California residence. Indoor Air 28, 572–584 (2018).
[5] Shinohara, N., Kataoka, T., Takamine, K. & Gamo, M. Distribution and variability of the 24-h average air exchange rates and interzonal flow rates in 26 Japanese residences in 5 seasons. Atmos Environ 45, 3548–3552 (2011).